European Commission

JRC TECHNICAL REPORTS

Study of a compact NRA system

Report prepared as part of the INFN – JRC collaboration agreement

Stefan Kopecky
Jan Heyse
Pierfrancesco Mastinu
Carlos Paradela
Peter Schillebeeckx

2016

Joint Research Centre

EUR 28245 EN

JRC Science Hub
https://ec.europa.eu/jrc

JRC103785

EUR 28245 EN

ISBN 978-92-79-63912-8

ISSN 1831-9424

doi:10.2787/867107

How to cite: S. Kopecky, J. Heyse, P. Mastinu, C. Paradela, P. Schillebeeckx; Study of a compact NRA system; EUR 28245 EN; doi:10.2787/867107

Study of a compact NRA system

S. Kopecky[a], J. Heyse[a], C. Paradela[a], P. Mastinu[b], P. Schillebeeckx[a]

[a]European Commission, Joint Research Centre,
Retieseweg 111, B - 2440 Geel, Belgium

[b]Laboratori Nazionali di Fisica Nucleare, Laboratori Nazionali di Legnaro
Viale dell'Università 2, I-35020 Legnaro, Italy

Table of contents

Abstract

A compact system for Neutron Resonance Analysis has been studied based on results of simulations. The influence of the moderator characteristics of the neutron producing target on both the neutron emission spectrum and the time-of-flight response functions has been investigated. Results obtained with different moderator geometries and materials have been compared. In addition, the transmission through a complex sample was simulated to verify the impact of the moderator thickness and pulse width on the observed resonance transmission profiles. Results have been validated by a comparison with experimental transmission data obtained from measurements at a 10 m transmission station of GELINA.

The results of this study reveal that the response functions and the energy dependence of the neutron spectrum are almost independent of the energy of initial neutrons. The absolute intensity decreases with increasing initial neutron energy. The best results are obtained when the face of the moderator viewing the flight path is flat. As expected, the moderator geometry, material and thickness have a strong impact on the response functions and on both the energy dependence and absolute intensity of the neutron spectrum. Schemes to optimise the moderator thickness and initial pulse width are presented.

1 Introduction

The presence of resonance structures in neutron induced reaction cross sections is the basis for Neutron Resonance Transmission Analysis (NRTA) and Neutron Resonance Capture Analysis (NRCA) [1]. NRTA and NRCA are Non-Destructive Analysis (NDA) methods to determine the elemental and isotopic composition of materials and object. Both methods are non-invasive and do not require any sample preparation. They require a pulsed white neutron source combined with Time-Of-Flight (TOF) measurements and rely on well-established methodologies for neutron interaction cross section measurements [2]. NRTA and NRCA can be used for a variety of applications in diverse fields, such as archaeological studies, characterisation of reference materials for cross section measurements, temperature measurements, study of fundamental properties of materials and characterisation of nuclear materials for nuclear safeguards and security [1].

NRTA is an absolute NDA technique. It can be considered as a complementary or even alternative analytical technique to Destructive Analysis (DA) when uncertainties in the order of 1 – 2% are required. Therefore, NRTA has been proposed as a method to quantify Special Nuclear Materials (SNM), i.e. Pu-isotopes and ^{235}U, in debris of melted fuel formed in a severe nuclear accident [3], such as the one that occurred at the Fukushima Daiichi power plants. NRCA can be applied as a complementary technique to identify and quantify impurities.

At the moment NRTA and NRCA are applied at relatively large TOF facilities such as the GELINA facility of the Joint Research Centre (JRC) in Geel (Belgium) [4] and the J-PARC facility of the Japan Atomic Energy Agency (JAEA) in Tokai-mura (Japan) [5]. For industrial applications a more compact facility is required. This study concentrates on the design specifications of a compact pulsed white neutron source, taking into account the requirements defined in Ref. [6]. These requirements are tailored for the characterisation of nuclear materials including complex materials such as spent nuclear fuel pellets and debris of melted fuel produced after a severe nuclear accident.

2 Impact of the moderator characteristics on the neutron intensity and TOF response function

For Neutron Resonance Analysis (NRA) measurements a pulsed white neutron source combined with the TOF-technique is required. This kind of facilities are based on a pulsed charged particle accelerator. The charged particle beam impinges on a target, in which neutrons can be produced by either two-body nuclear reactions, photonuclear reactions or the spallation process. Evidently only those based on two-body and photonuclear reactions are an option for a compact system [7]. Neutron spectra originating from two-body reactions [8], e.g. ^{7}Li(p,n), ^{9}Be(p,n) or ^{3}H(d,n), and photonuclear reactions, e.g. ^{9}Be(γ,n), ^{2}H(γ,n) or photonuclear reaction in heavy materials, do not cover the epi-thermal or thermal energy region. Therefore, to create a white neutron source covering the resonance region, a moderator is required. The characteristics of the moderator will have an influence on both the neutron spectrum and the response function for TOF-measurements.

Response functions R(t,E) of a TOF-spectrometer express the probability that a neutron with energy E is observed with a time-of-flight t. Such functions can be considered as a convolution of different independent components due to [2]:

- the finite duration of the accelerator start pulse (Δt_0),
- the time resolution of the detectors and electronics (Δt_s),
- the neutron transport in the neutron producing target-moderator assembly (Δt_t), and
- the neutron transport in the detector or sample (Δt_d).

The broadening due to the target-moderator assembly (Δt_t) is mostly the main component [2]. This broadening strongly depends on the neutron physics properties and geometry of the moderator. For practical reasons response functions due to the neutron transport are better represented by introducing an equivalent distance, as discussed in detail in Refs. [1] and [2]. The equivalent distance L_t is defined by $L_t = v\ t_t$, where t_t is the time difference between the moment the neutron leaves the target-moderator assembly and its time of creation. Such a transformation of variables results in distributions that are almost independent of the energy of the neutron escaping from the target-moderator assembly [1],[2].

2.1 Moderator thickness

To study the influence of the moderator thickness on the spectrum of the neutrons escaping from the moderator $\varphi(E)$ and on the TOF-response $R(L_t,E)$, Monte Carlo simulations using a water moderator in a spherical geometry were performed. The simulations were performed with the MCNP 4 C code. The geometry is shown in Figure 1. The neutron spectra and response functions were determined starting from a mono-energetic isotropic neutron source placed in the centre of the sphere. The response function was derived for neutrons escaping from the moderator with an energy E between 1 eV and 100 eV.

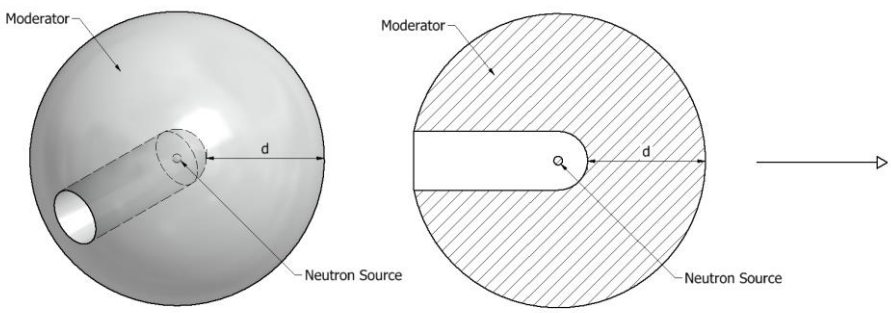

Figure 1 Schematic representation of a water moderator in a spherical geometry. The arrow indicates the direction of the neutron beam considered in the calculations.

The neutron energy spectra $\varphi(E)$ for initial neutron energies E_0 = 100 keV and E_0 = 14 MeV are shown in Figure 2 for a spherical water moderator with shell thickness d = 1 cm, 2 cm, 3 cm and 4 cm. The corresponding response functions $R(L_t, E = 1\ eV - 100\ eV)$ for d = 2 cm and 4 cm are compared in Figure 3. These figures illustrate that both the energy spectra and response functions strongly depend on the moderator thickness.

However, for a fixed moderator thickness the shape of the neutron spectrum (or its energy dependence) and the response function in terms of equivalent distance are almost independent of the initial neutron energy in the neutron energy region under consideration (1 eV – 100 eV). This is confirmed in Figure 3 and Figure 4. The latter compares for a spherical water moderator with shell thickness d = 2 cm the neutron spectrum obtained with initial neutron energies E_0 = 50 keV, 500 keV, 2 MeV and 14 MeV. The resolution is directly related to the moderator thickness and almost independent from the initial neutron energy. For a moderator thickness d = 2 cm and 4 cm the resolution expressed in Full Width at Half Maximum (FWHM) is FWHM ≈ 2.2 cm and ≈ 3.2 cm, respectively.

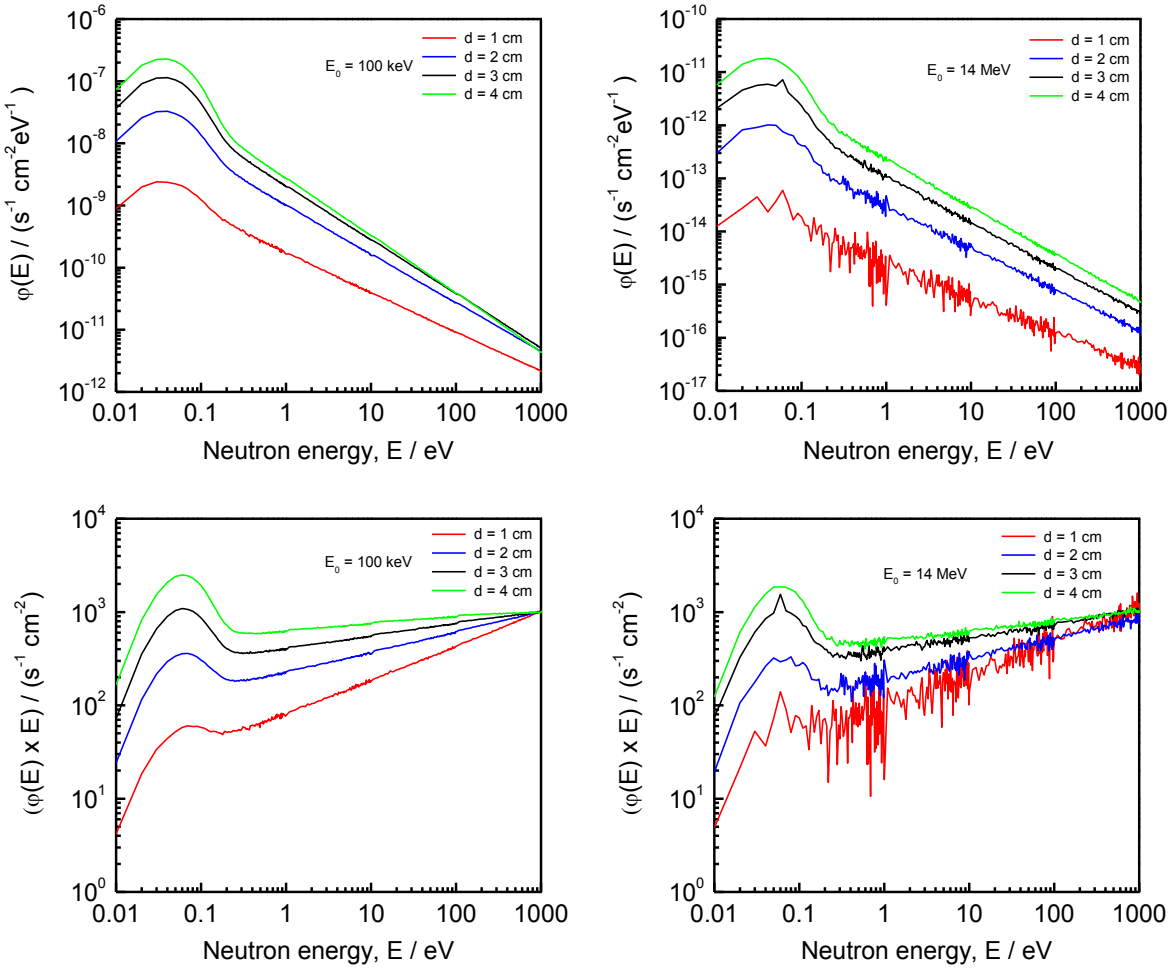

Figure 2 Energy spectra of neutrons escaping from a spherical water moderator with a shell thickness d = 1 cm, 2 cm, 3 cm and 4 cm. The spectra are shown for an initial neutron energy E_0 = 100 keV (left) and E_0 = 14 MeV (right). The figures on top show the absolute neutron spectra for an isotropic neutron source with an intensity of one neutron per second. The spectra below are multiplied with the energy (lethargy spectra) and normalised to 1000 $s^{-1}cm^{-2}$ at 1000 eV. The spectra for E_0 = 14 MeV suffer from Monte Carlo counting statistics effects.

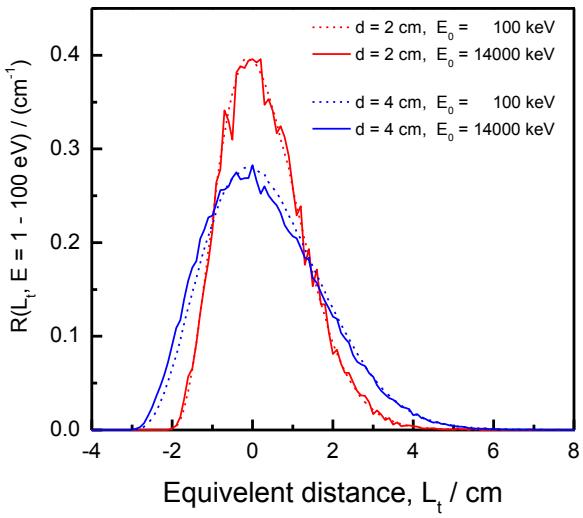

Figure 3 Response functions $R(L_t, E = 1 - 100\ eV)$ for a spherical water moderator with a shell thickness d = 2 cm and 4 cm. Response functions are given for an initial neutron energy E_0 = 100 keV and E_0 = 14 MeV.

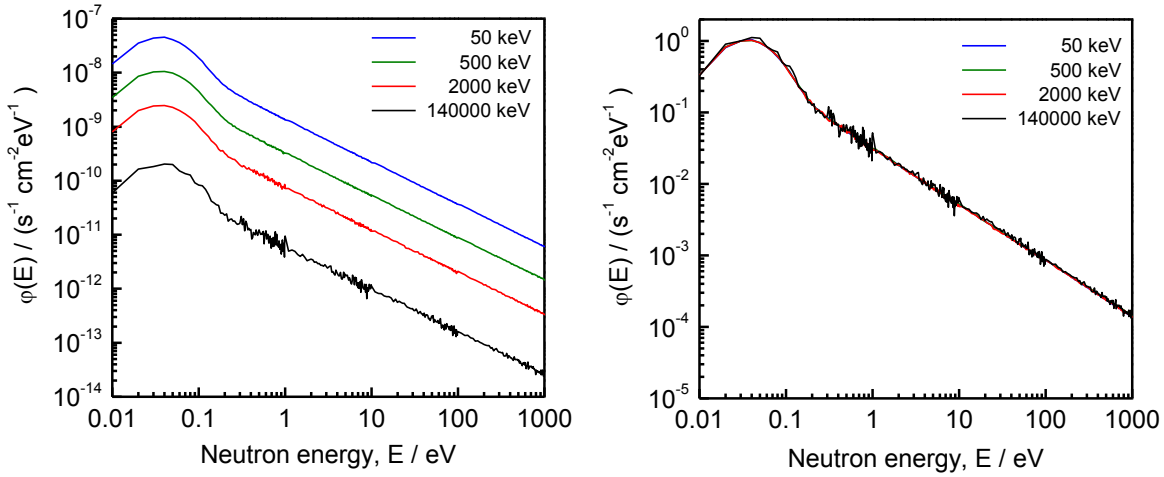

Figure 4 Energy spectra of neutrons escaping from a spherical water moderator with a shell thickness d = 2 cm. The spectra are shown for an initial neutron energy E_0 = 50 keV, 500 keV, 2 MeV and 14 MeV. The figure on the left compares the absolute neutron spectra for an isotropic neutron source with an intensity of one neutron per second. The spectra on the right are normalised to 1 $s^{-1}cm^{-2}\ eV^{-1}$ at 40 meV.

The absolute intensity of the neutron spectrum depends on both the initial neutron energy and the moderator thickness. This is illustrated in Figure 5 and Figure 6. The dependence on the moderator thickness for an initial neutron energy E_0 = 100 keV and 14 MeV is shown in Figure 5. These data reveal that for E_0 = 100 keV the intensity reaches a maximum at d ≈ 4 cm. For E_0 = 14 MeV more than 10 cm shell thickness is needed to reach the maximum. In Figure 6, the intensity for a neutron that escapes from a 2 cm thick spherical water moderator with an energy E = 10 eV is plotted as a function of the initial neutron energy. The intensity drops by almost a factor 100 going from an initial neutron energy of E_0 = 0.1 MeV to 10 MeV.

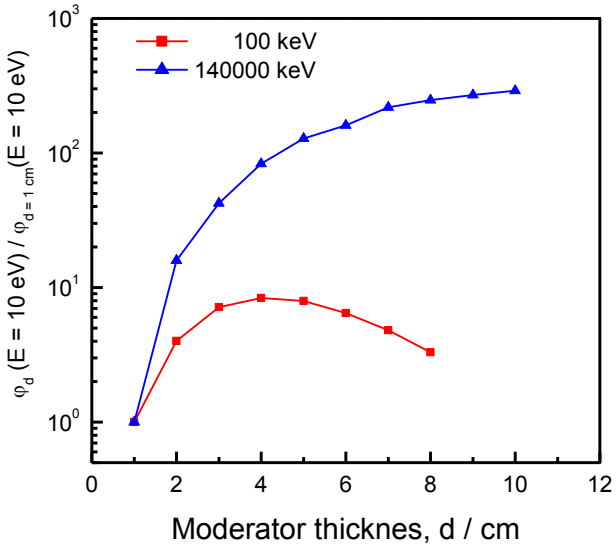

Figure 5 Relative intensity of the neutron flux φ(E = 10 eV) as a function of the shell thickness of a spherical water moderator. The intensity is given for an initial neutron energy of E_0 = 100 keV and E_0 = 14 MeV and compared to the intensity at d = 1 cm.

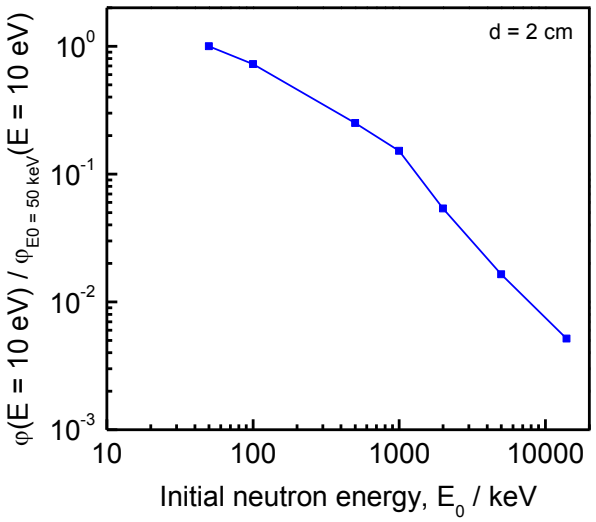

Figure 6 Relative intensity of the neutron flux φ(E = 10 eV) as a function of initial neutron energy E_0. The intensity is calculated for a spherical water moderator with shell thickness d = 2 cm and normalised to 1 at E_0 = 50 keV.

2.2 Moderator geometry

The impact of the moderator geometry was verified by comparing the neutron flux $\varphi(E)$ and response functions $R(L_t,E)$ obtained with the spherical geometry (Figure 1) and those for a cylindrical geometry (Figure 7). For the two geometries the thickness of the moderator side viewing the flight path is d = 2 cm. The surface of the moderator viewing the flight path is flat in the cylindrical geometry. The calculations were performed for an initial neutron energy E_0 = 500 keV. The neutron spectrum $\varphi(E)$ and response function $R(L_t,E)$ were calculated for a neutron beam escaping from the moderator in the direction indicated by the arrow.

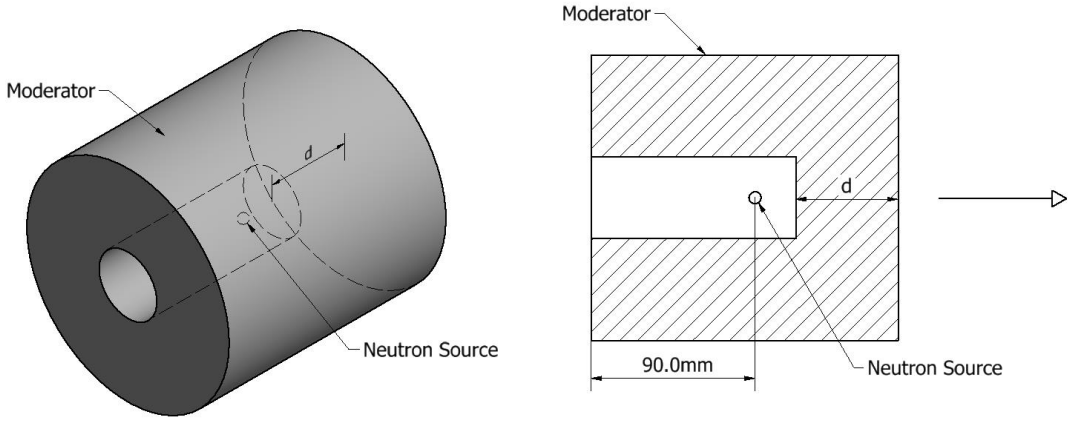

Figure 7 Schematic representation of a moderator in a cylindrical geometry. The arrow indicates the direction of the neutron beam considered in the calculations.

The results in Figure 8 and Figure 9 show that for a given thickness d the cylindrical geometry is a more favourable configuration compared to the spherical geometry. The absolute neutron intensity is systematically higher for the cylindrical geometry. In addition, a better resolution is obtained: the FWHM is reduced from a FWHM ≈ 2.5 cm in spherical geometry to a FWHM ≈ 2.0 cm in cylindrical geometry and the distribution approaches more a χ^2 distribution as expected from theoretical considerations [9].

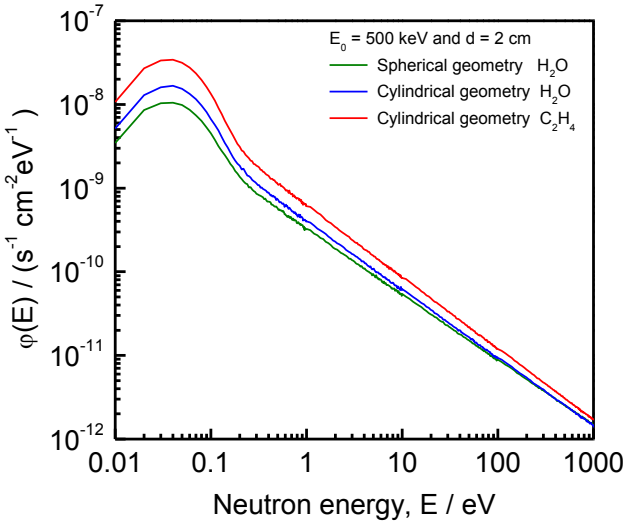

Figure 8 Neutron spectrum $\varphi(E)$ for a water moderator in spherical (see Figure 1) and cylindrical (see Figure 7) geometry. The spectrum for a polyethylene (C_2H_4) moderator in cylindrical geometry is also shown. The results are obtained for an initial neutron energy E_0 = 500 keV.

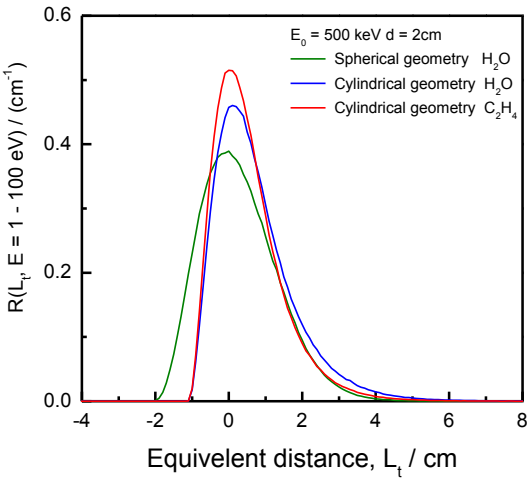

Figure 9 Response function $R(L_t, E = 1 - 100\ eV)$ for a H_2O moderator in spherical (Figure 1) and cylindrical (Figure 7) geometry. The result for a C_2H_4 moderator in cylindrical geometry is also shown. The responses are given for an initial neutron energy $E_0 = 500$ keV.

2.3 Moderator material

The impact of the moderator material was verified by comparing the neutron flux $\varphi(E)$ and response function $R(L_t,E)$ obtained with the cylindrical geometry in Figure 7 using polyethylene (C_2H_4) and water (H_2O) as moderating material. The calculations were performed for an initial neutron energy $E_0 = 500$ keV and a moderator thickness d = 2 cm. The results in Figure 8 reveal a small difference in the energy dependence. The absolute neutron intensity is slightly higher using C_2H_4 as moderator material. The resolution for a C_2H_4 moderator (FWHM ≈ 1.8) is better compared to the one for H_2O moderator (FWHM ≈ 2.0).

2.4 Comparison with the GELINA moderator

Additional simulations were performed using a H_2O moderator in a geometry which is similar to one at GELINA [4]. This configuration is shown in Figure 10. The thickness of the moderator side viewing the flight path is d = 3.7 cm.

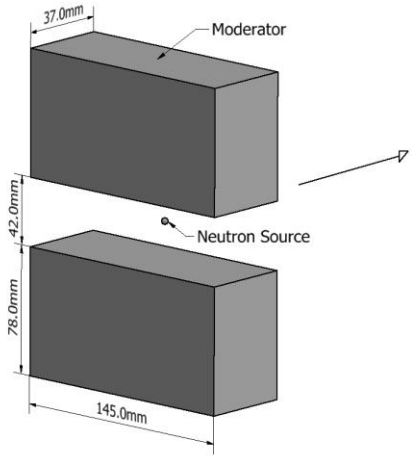

Figure 10 Schematic representation of a H_2O moderator with a geometry similar to the one at the GELINA facility [4]. The arrow indicates the direction of the neutron beam considered in the calculations.

The neutron flux $\varphi(E)$ and response function $R(L_t, E = 1 - 100\ eV)$ for this configuration and those for a C_2H_4 moderator in cylindrical configuration are compared in Figure 11 and Figure 12, respectively. The results are for an initial neutron energy E_0 = 500 keV. For the cylindrical geometry the flux is shown for d = 4 cm. The response for the cylindrical geometry is given for d = 1 cm, 2 cm, 3 cm and 4 cm. These figures show small differences in the energy dependence of the neutron flux. The intensity in the cylindrical geometry is increased by about a factor 2 compared to the one for the GELINA configuration. The calculated flux is also compared with an experimental one resulting from measurements at a measurement station of GELINA. The absolute calculated flux is consistent with a total primary neutron emission rate of 2.5×10^{13} s^{-1}, which is the nominal emission rate at GELINA with the accelerator operating at 60 μA. The response function $R(L_t,E)$ in the GELINA geometry is very similar to the one in cylindrical geometry with d = 3 cm.

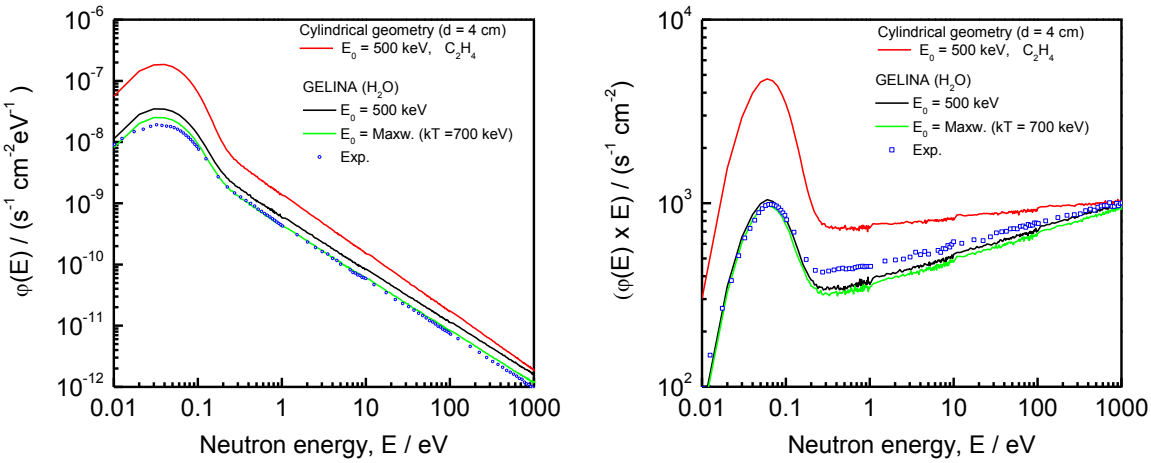

Figure 11 Energy spectra of neutrons escaping from a C_2H_4 moderator in cylindrical geometry with d = 4 cm and a H_2O moderator in a configuration similar to the one of GELINA. The results are for an initial neutron energy E_0 = 500 keV. For the GELINA geometry the flux for an initial Maxwellian energy spectrum, with kT = 700 keV, is also given and compared with an experimental spectrum taken at GELINA [12]. The figure on the left compares the absolute neutron spectra for an isotropic neutron source with an intensity of one neutron per second. The spectra on the right are multiplied with the energy (lethargy spectra) and normalised to 1000 $s^{-1}cm^{-2}$ at 1000 eV.

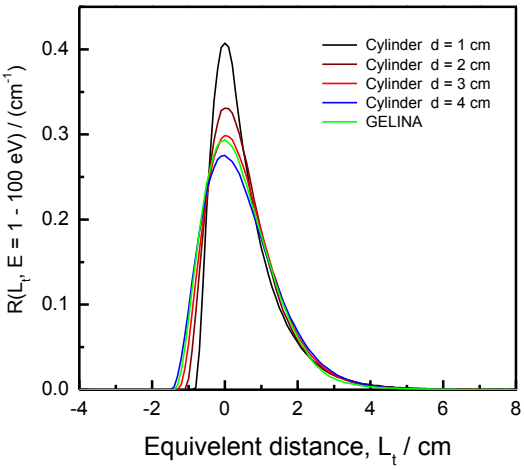

Figure 12 Response function $R(L_t, E = 1 - 100\ eV)$ for a C_2H_4 moderator in cylindrical (Figure 7) geometry and a H_2O moderator in a GELINA geometry (Figure 10). The results are for an initial neutron energy E_0 = 500 keV. For the cylindrical geometry results are given for d = 1 cm, 2 cm, 3 cm and 4 cm.

3 Transmission through complex materials

To design and optimise the characteristics of a neutron source for a compact NRA measurement system a compromise between neutron intensity and resolution has to be made. In Ref. [6] the basic requirements of a NRA system for nuclear safeguards and security applications were defined based on measurements at GELINA. From this study one concludes that an overall relative TOF-resolution of about $\Delta E/E \approx 0.008$ is a minimum requirement. This condition defines constraints on the moderator thickness and initial pulse width.

This constraint was verified for a C_2H_4 cylindrical moderator by calculating the transmission through a sample consisting of B_4C, Co, Mn, Nb, Rh, and W, which was used for NRTA measurements at GELINA. For this calculation, the REFIT code was used. The sample, which was used for NRTA measurements at an 11.8 m transmission station of GELINA [11], creates a complex transmission with overlapping transmission dips and a substantial flux reduction due to matrix material without resonances in the low energy region.

The transmission through this sample resulting from measurements at GELINA is shown in Figure 13. It is compared with a theoretical transmission based on a H_2O cylindrical moderator with d = 4 cm, an initial pulse width Δt_0 = 100 ns and a flight path with length L = 10 m. The results in Figure 13 show that the resolution for the cylindrical geometry with d = 4 cm, Δt_0 = 100 ns and L = 10 m is sufficient to analyse such a complex transmission. A similar resolution can be obtained for a H_2O cylindrical moderator with d = 1 cm, 2 cm and 3 cm, however, with flight path lengths L = 2.5 m, 5.0 m and 7.5 m and pulse widths Δt_0 = 25 ns, 50 ns and 75 ns, respectively. An additional constraint is related to the operating frequency to limit the overlap neutron energy to ~ 0.5 eV. Under this condition the background due to overlap neutrons is largely reduced by inserting a Cd-overlap filter in the beam. These conditions are summarised in Table 1. The relative intensity of the neutron flux at 10 eV per primary neutron as a function of the moderator thickness is shown in Figure 14. The corresponding relative intensity, considering the operational conditions in Table 1 and supposing a pure isotropic neutron emission rate, i.e. directly proportional to L^{-2}, is listed in the last column of Table 1. These data show that the constraints can also be fulfilled at a shorter distance with an increase in intensity by a factor 2.5.

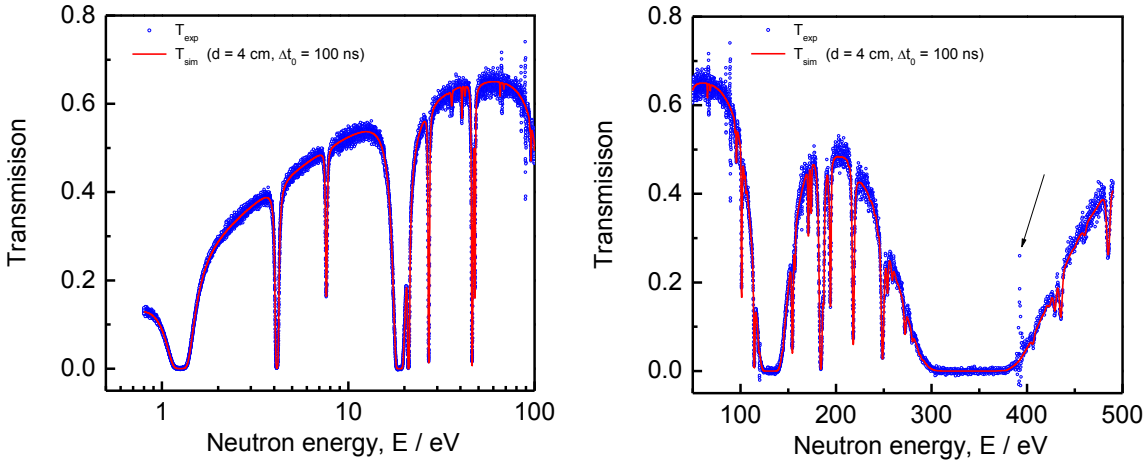

Figure 13 Transmission through a sample consisting of B_4C, Co, Mn, Nb, Rh, and W. Results of a measurement at a 10 m station of GELINA are compared with a theoretical transmission for a neutron beam escaping from a H_2O cylindrical moderator with thickness d = 4 cm and a flight path length L = 10 m.

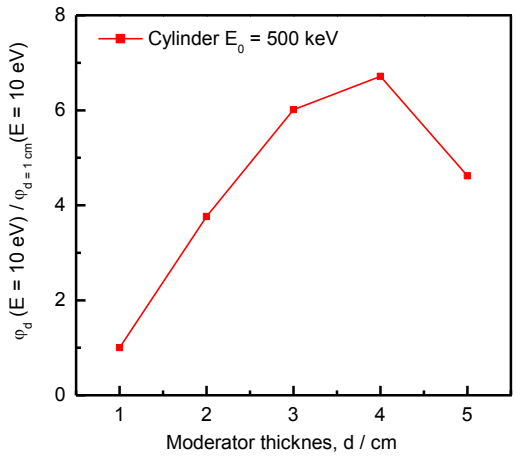

Figure 14 Neutron flux at 10 eV as a function of the moderator thickness for a H_20 moderator in cylindrical geometry and an initial neutron energy E_0 = 500 keV. The flux is normalised to 1 at d = 1 cm.

L / m	d / cm	Δt_0 / ns	f_M	I_L / $I_{L=10m}$
2.5	1	25	3950	2.5
5.0	2	50	1950	2.3
7.5	3	75	1300	1.6
10.0	4	100	950	1

Table 1 Flight path distance L, moderator thikcness d, initial pulse width and maximum operating frequency f_M to fulfill the constraints of Ref. [11], i.e. a minimum relative energy resolution $\Delta E/E \approx 0.008$ and maximum overlap energy of 0.5 eV. The resulting intensities, normalised to one for the conditions for a flight path length L = 10 m, are given in the last column.

For a given flight path length the moderator thickness and initial pulse width can be optimised taking into account the reduction in intensity with decreasing moderator thickness and the proportionality between pulse width and intensity. The transmissions through the complex sample for L = 10 m and a cylindrical moderator with thickness d = 2 cm and 4 cm and initial pulse widths Δt_0 = 10 ns and 100 ns are compared in Figure 15. Only for energies above 450 eV the effect of an improved resolution due to a reduction in moderator thickness and pulse width is observed. However, initial pulse widths Δt_0 = 1000 ns and Δt_0 = 10000 ns are not suitable to determine the composition of complex samples by NRTA for a flight path length L = 10 m. This is illustrated in Figure 16, which compares the transmissions for d = 4 cm and L = 10 m and initial pulse widths Δt_0 = 10 ns, 100 ns, 1000 ns and 10000 ns.

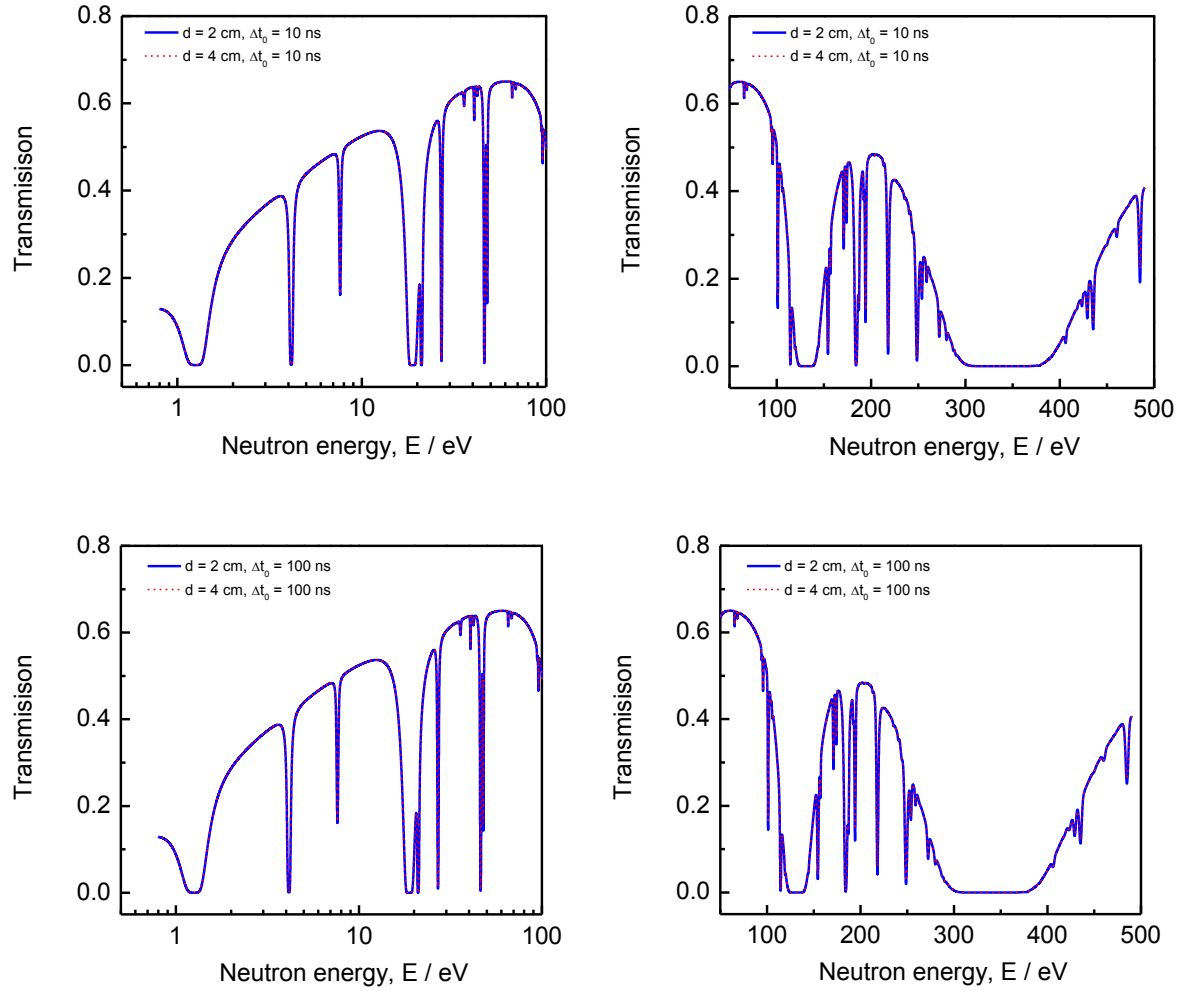

Figure 15 Transmissions through a sample consisting of B_4C, Co, Mn, Nb, Rh, and W. The transmissions are calculated for flight path length L = 10 m and a H_2O cylindrical moderator with thicknesses d = 2 cm and 4 cm and initial pulse widths Δt_0 = 10 ns (top) and 100 ns (bottom).

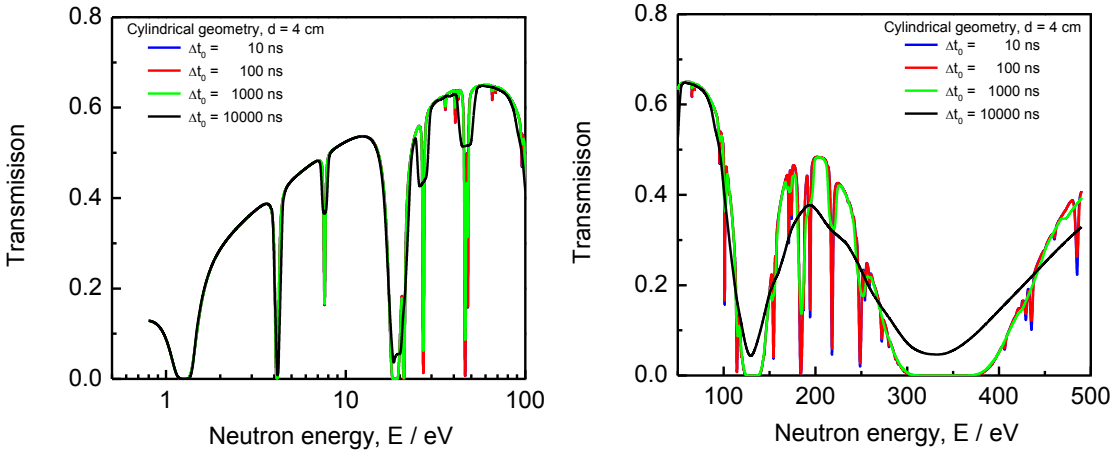

Figure 16 Transmissions through a sample consisting of B_4C, Co, Mn, Nb, Rh, and W. The transmissions are calculated for flight path length L = 10 m and a H_2O cylindrical moderator with thickness d = 4 cm and initial pulse widths Δt_0 = 10 ns, 100 ns, 1μs and 10 μs.

4 Summary and conclusions

The impact of the moderator characteristics and initial pulse width on the neutron emission spectrum and the TOF-response function for NRA applications was studied. The data reveal that the shape of the neutron spectrum (or its energy dependence) and the response function are almost independent of the initial neutron energy. However, the absolute intensity strongly depends on the moderator thickness and initial neutron energy. As expected the resolution due to the neutron transport in the moderator is directly related to the moderator thickness.

The results of this study reveal that the best results in terms of both intensity and resolution are obtained when the face of the moderator viewing the flight path is flat. In case a facility with multiple beam lines is planned the cylindrical geometry can be improved by making all surfaces viewing the beam lines flat.

A study of the transmission through a complex sample, resulting in a complex resonance transmission profile, reveals that the moderator thickness and flight path distance can be optimised to increase the intensity and maintaining the constraints required for the analysis of complex transmission profiles.

References

[1] P. Schillebeeckx, B. Becker, H. Harada and S. Kopecky, "Neutron resonance spectroscopy for the characterisation of materials and objects", JRC Science and Policy Reports, Report EUR 26848-EN (2014).

[2] P. Schillebeeckx, B. Becker,Y. Danon, K. Guber, H. Harada, J. Heyse, A.R. Junghans, S. Kopecky, C. Massimi, M.C. Moxon, N. Otuka, I. Sirakov and K. Volev, "Determination of resonance parameters and their covariances from neutron induced reaction cross section data", Nuclear Data Sheets 113 (2012) 3054 – 3100.

[3] H. Harada, F. Kitatani, M. Koizumi, H. Tsuchiya, J. Takamine, M. Kureta, H. Iimura, M. Seya, B. Becker, S. Kopecky and P. Schillebeeckx, "Proposal of Neutron Resonance Densitometry for Particle Like Debris of Melted fuel using NRTA and NRCA", Proceedings of the 35th ESARDA symposium on Safeguards and Nuclear Non-Proliferation, 28 – 30 May 2013, Brugge (Belgium)

[4] W. Mondelaers and P. Schillebeeckx, "GELINA, a neutron time-of-flight facility for neutron data measurements", Notiziario Neutroni e Luce di Sincrotrone 11 (2006) 19 – 25.

[5] H. Hasemi, M. Harada, T. Kai, T. Shinohara, M. Ooi, H. sato, K. Kino, M. Segawa, T. Kamiyama and Y. Kiyanagi, "Evaluation of nuclide density by neutron transmission at the NOBORU instrument in J-PARC/MLF", Nuclear Instruments and Methods in Physics Research A 773 (2015) 137 – 149.

[6] C. Paradela, G. Alaerts, J. Heyse, S. Kopecky, L. Salamon, P. Schillebeeckx, R. Wynants, H. Harada, F. Kitatani, M. Koizumi and H. Tsuchiya, "Neutron Resonance Analysis System Requirements", JRC Technical Reports, Report EUR 28239 EN

[7] M. Uesaka and H. Kobayasgi, "Compact Neutron Sources for Energy and Security", Reviews of Accelerator Science and Technology 8 (2015) 181 – 207.

[8] M. Drosg, "Monoenergetic neutron production by two-body reactions in the energy range from 0.0001 to 500 MeV. An overview", IAEA Technical Consultants Meeting on Accelerator-Based Neutron Sources, KFKI, Debrecen, Hungary, October 1999.

[9] H. J. Groenewold and H. Groendijk, "Non-thermal neutron cascade", Physica XIII (1947) 141 – 152.

[10] M.C. Moxon and J.B. Brisland, Technical Report AEA-INTEC-0630, AEA Technology (1991).

[11] C. Paradela, G. Alaerts, B. Becker, H. Harada, J. Heyse, F. Kitatani, M. Koizumi, S. Kopecky, W. Mondelaers, A. Moens, P. Schillebeeckx, H. Tsuchiya and R. Wynants, "NRD Demonstration Experiments at GELINA", JRC Technical Report, Report EUR 27507 EN (2015).

[12] M. Flaska, A. Borella, D. Lathouwers, L.C. Mihailescu, W. Mondelaers, A.J.M. Plompen, H. van Dam, T.H.J.J. van der Hagen, "Modeling of the GELINA neutron target using coupled electron–photon–neutron transport with the MCNP4C3 code", Nuclear Instruments and Methods in Physics Research A 531 (2004) 392–406

List of abbreviations and definitions

EC	European Commission
DA	Destructive Analysis
FWHM	Full Width at Half Maximum
GELINA	Geel Electron LINear Accelerator
JAEA	Japan Atomic Energy Agency
J-PARC	Japan Proton Accelerator Research Complex
JRC	Joint Research Centre
NDA	Non-Destructive Analysis
NRA	Neutron Resonance Analysis
NRCA	Neutron Resonance Capture Analysis
NRM	Nuclear Reference Material
NRTA	Neutron Resonance Transmission Analysis
RSA	Resonance Shape Analysis
SNM	Special Nuclear Material
TOF	Time-Of-Flight

List of figures

List of tables

LA-NA-28245-EN-N

JRC Mission

As the Commission's in-house science service, the Joint Research Centre's mission is to provide EU policies with independent, evidence-based scientific and technical support throughout the whole policy cycle.

Working in close cooperation with policy Directorates-General, the JRC addresses key societal challenges while stimulating innovation through developing new methods, tools and standards, and sharing its know-how with the Member States, the scientific community and international partners.

Serving society
Stimulating innovation
Supporting legislation

doi:10.2787/867107

ISBN 978-92-79-63912-8